Synthesis, X-ray structure, spectroscopic properties and DFT studies of some dithiocarbazate complexes of nickel(II)

Reza Takjoo [a,*], Roberto Centore [b,*]

[a] Department of Chemistry, School of Sciences, Ferdowsi University of Mashhad, Mashhad 91775-1436, Iran
[b] Department of Chemical Sciences, University of Naples "Federico II", Via Cinthia, I-80126 Naples, Italy

HIGHLIGHTS

► Two nickel(II) dithiocarbazate complexes are synthesized.
► The nickel(II) complexes were prepared and characterized by spectral techniques.
► The structures of compounds are determined by X-ray studies.
► The complexes show distorted square planar geometries.
► The DFT calculations for the optimization, Mulliken charge, FMO and NBO are done.

ARTICLE INFO

ABSTRACT

Two nickel(II) complexes with formulae NiL_2 (**1**) and NiL'Im (**2**) (HL = allyl 2-benzylidene-hydrazinecarbodithioate, H_2L' = allyl 2-(2-hydroxybenzylidene)hydrazinecarbodithioate, Im = Imidazole) have been synthesized and characterized by elemental analysis, molar conductivities, FT-IR, ^{1}H NMR and UV/Vis spectroscopy. The crystal structure of the complexes has been determined by single crystal X-ray diffractometry. Both L and L' ligands are coordinated to the metal in the thiolate form. In **1**, the square planar coordination of the metal is achieved by coordination of two bidentate ligand units acting through azomethine nitrogen and the thiolato sulfur donor atoms. The complex **2** has a square-planar geometry with the tridentate ligand coordinated to the metal through salicylate oxygen, azomethine nitrogen and the thiolato sulfur atoms, while the fourth coordination position is occupied by one N atom of imidazole. Also natural bond orbitals (NBOs), frontier molecular orbitals (FMOs) and Mulliken charge computational studies on complexes carried out in the ground state with the DFT and theory at B3LYP/6-31G(d,p) level of theory.

1. Introduction

During the past years, the synthesis of new coordination compounds containing nitrogen and sulfur donor atoms has been significantly developed. Among these materials, dithiocarbazate compounds have been specifically considered by researchers because of biological properties such as antibacterial [1], antimalarial [2], antiviral [3], antitumor [4,5], insecticidal [6] and optoelectronic properties such as good non-linear optical (NLO) response [7]. Actually, dithiocarbazates constitute one of the most important classes of mixed hard–soft nitrogen–sulfur donor ligands [8,9]. A change in the substitution pattern of these compounds can create new ligands with different properties.

In dithiocarbazate compounds, owing to thione–thiol tautomery, N and S donor atoms are connected to the metal ion with the formation of five- or six-member rings. The presence of additional donor atoms in suitable position in the compound can increase the coordination ability of the ligand giving rise to different coordination geometries [10].

The transition metal complexes of dithiocarbazates have different geometric, electronic, optical [11], magnetic [12], semiconducting [13] and radiopharmaceutical properties as well [14].

In particular, planar nickel(II) complexes are coordinatively unsaturated and can act as Lewis acids [15]; the anticancer [16] and antimicrobial [17] activity of many nickel complexes, as well as their NLO performances [18], may be related with that feature.

In order to study allyl group effects on the physico-chemical properties of dithiocarbazates, we report here the synthesis, characterization and X-ray crystal structures of two new complexes bis(allyl-2-(phenylmethylene)hydrazinecarbothioamido)nickel(II)

* Corresponding authors. Tel./fax: +98 511 8975457.
E-mail addresses: rezatakjoo@yahoo.com (R. Takjoo), roberto.centore@unina.it (R. Centore).
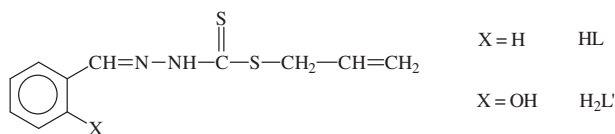
Scheme 1. Chemical diagrams of the ligand precursors.

(NiL$_2$) and [allyl-2-(2-hydroxyphenyl)methylene]hydrazinecarbothioamido)-imidazole-nickel(II) (NiL′Im) where HL, H$_2$L′ and Im are, respectively, allyl 2-benzylidenehydrazinecarbodithioate (HL), allyl 2-(2-hydroxybenzylidene)hydrazinecarbodithioate (H$_2$L′) and imidazole, see Scheme 1.

Moreover, we also present the DFT calculations to investigate the geometry, electronic structure atomic charge distributions and bond analysis of the complexes.

2. Experimental

2.1. Reagents

All the material were purchased form Merck Chemical Company and were used as received. All solvents were reagent grade and used without further purification. Allyl 2-benzylidene-hydrazine-carbodithioate (HL) and allyl 2-(2-hydroxybenzylidene) hydrazine-carbodithioate (H$_2$L′) were prepared by previously reported procedures [8,19].

2.2. Physical measurements

C, H, N, S elemental analyses were performed using a Thermo Finnigan Flash 1112EA elemental analyzer. The IR spectra in the range 4000–400 cm^{-1} were recorded from KBr pellets using a Buck 500 Scientific spectrometer. The mass spectra were recorded on a MAT CH7A. Proton NMR spectra were recorded on a Bruker BRX 100 AVANCE spectrometer with TMS as internal standard. The electronic spectra were recorded in DMF with a SHIMADZU model 2550 UV–Vis spectrophotometer (260–900 nm). The molar conductance values of 10^{-3} M DMF solutions of the complexes were measured with a Metrohm 712 Conductometer.

2.3. Synthesis of bis(allyl-2-(phenylmethylene)hydrazinecarbothioamido)nickel(II) (1)

Nickel(II) chloride hexahydrate (0.2 g, 1 mmol) in boiling ethanol (10 mL) was added to the ethanol solution (10 mL) of the HL ligand precursor (0.48 g, 2 mmol). The mixture was heated in a water bath for 30 min and then left to stand overnight. The brown product was filtered off, washed with ethanol and dried in a vacuum desiccator over anhydrous silica gel. The complex was recrystallized from DMF/ethanol to obtain diffraction quality crystals.

Yield: 0.30 g, 56%. m.p.: 140 °C. Molar conductance (10^{-3} M, DMF) 2.5 ohm^{-1} cm^2 mol^{-1}. Anal. Calc. for C$_{22}$H$_{22}$N$_4$NiS$_4$ (529.39 g mol^{-1}): C, 52.35; H, 4.97; N, 11.10; S, 25.41; Ni, 11.09. Found: C, 52.58; H, 4.78; N, 11.07; S, 24.94; Ni, 10.68%. IR (KBr) cm^{-1}: ν(C=C) 1640w, ν(C=N) 1595 m, ν(C=C$_{ring}$) 1487w, ν(C=N + C=S) 1178 m, ν(N—N) 1025s, ν(C—S) 950 m. ^{1}H NMR (100 MHz, CDCl$_3$, 25 °C, ppm): δ = 3.8 (d, 2H; C9), 5.1–5.4 (dd, 2H; C11), 5.7–6.2 (m, 1H: C10), 7.4–7.8 (m, 5H; ring), 8.1 (s, 1H; C7). UV/Vis (CHCl$_3$) λ_{max}, nm (logε, L mol^{-1} cm^{-1}): 256(4.40), 285(4.47), 317(4.45), 450(4.95).

2.4. Synthesis of [allyl-2-(2-hydroxyphenyl)methylene] hydrazinecarbothioamido)imidazole-nickel(II) (2)

A solution of nickel(II) acetate tetrahydrate (0.4 g, 0.4 mmol) in ethanol (5 mL) was mixed with a solution of the H$_2$L′ ligand precursor (0.1 g, 0.4 mmol) in the same solvent (5 mL) and the green solution was heated on a water bath for ca. 5 min whereupon a solution of imidazole (0.04 g; 0.6 mmol) in ethanol (5 mL) was added. The brown solution was heated on a water bath for 30 min and then left to stand overnight. The red crystalline product which formed after a week was filtered off, washed with ether and dried in a vacuum desiccator over anhydrous silica gel.

Yield: 0.04 g, 27%. m.p.: 187 °C. Molar conductance (10^{-3} M, DMF) 0.65 ohm^{-1} cm^2 mol^{-1}. Anal. Calc. for C$_{14}$H$_{14}$N$_4$NiOS$_2$ (317.11 g mol^{-1}): C, 44.59; H, 3.74; N, 14.86; S, 17.01; Ni, 15.56. Found: C, 43.85; H, 3.80; N, 14.76; S, 16.60; Ni, 14.89%. IR (KBr) cm^{-1}: ν(NH) 3053w, ν(C=N) 1595s, ν(C—O) 1525 m, ν(N—N) 1030s, ν(C—S) 960 m. ^{1}H NMR (100 MHz, CDCl$_3$, 25 °C, ppm): δ = 3.78 (d, 2H; C9), 5.26 (dd, 2H; C11), 5.8–6.2 (m, 1H; C10), 6.7–7.2 (m, 4H; phenol ring), 7.2–7.4 (m, 2H; C14, C13), 7.85 (s, 1H; C12), 8.14 (s, 1H; C7), 10.4 (bs, 1H; NH imidazole). UV/Vis (CHCl$_3$) λ_{max}, nm (logε, L mol^{-1} cm^{-1}): 243(4.38), 270(4.23), 383(4.03), 419(2.78).

2.5. X-ray structure determination

Single crystals of **1** and **2** suitable for X-ray analysis were grown from DMF. Data were collected on a Bruker-Nonius Kappa-CCD diffractometer using graphite monochromated MoKα radiation (λ = 0.71073 Å) at 173 K. Absorption correction was performed using the multi-scan method [20]. The structures were solved by direct methods [21] and refined by the full matrix least squares method [22] on F^2 against all reflections, using anisotropic displacement parameters for non-H atoms. The positions of H atoms were determined stereochemically, with exception for the N—H atoms of imidazole rings of **2**, whose positions were determined in difference Fourier maps. Refinement of H atoms was performed by the riding model with U_{iso} = 1.2U_{eq} of the carrier atom. In the case of **1** the investigated crystal specimens resulted twinned by rotation of 180° around the **b** axis. Many attempts to select a non-twinned specimen failed, so the X-ray analysis was eventually performed on a twinned sample. During the refinement, the twinning was handled with the TWIN instruction of the Shelxl package [22] using the proper rotation matrix ($-1\,0\,0/0\,1\,0/0\,0\,-1$) and assuming racemic twinning. That accounts for the higher final R

Table 1
Crystal, collection and refinement data for **1** and **2**.

Compound	1	2
Chem. formula	(C$_{11}$H$_{11}$N$_2$S$_2$)$_2$Ni	(C$_{14}$H$_{14}$N$_4$OS$_2$)Ni
Formula weight	529.39	377.12
T (K)	173(2)	173(2)
Crystal system	Monoclinic	Triclinic
Space group	P2$_1$/n	P − 1
a (Å)	4.243(1)	8.386(1)
b (Å)	19.284(8)	9.7680(7)
c (Å)	14.070(6)	19.052(3)
$\alpha/\beta/\gamma$ (°)	90/96.15(2)/90	86.221(8)/83.88(1)/76.071(8)
V(Å^3), Z	1145(1), 2	1504.8(3), 4
Density (g/cm^3)	1.536	1.665
Absorption coefficient	1.231 mm^{-1}	1.572 mm^{-1}
θ max	24.99°	27.5°
Indep. refl.	4523	6655
Data/param.	4523/142	6655/397
R, wR ($I > 2(I)$)	0.0987, 0.2482	0.0662, 0.1472
R, wR (all data)	0.1313, 0.2586	0.1068, 0.1566
Max. peak and hole (e/Å^3)	1.815, −0.743	0.708, −0.549

factors and residual electronic density. A summary of crystal, collection and refinement data is shown in Table 1.

2.6. Theoretical calculations

The gas phase geometry of all compounds was fully optimized using density functional theory (DFT) at the B3LYP/6-31G(d,p) basis set [23,24] levels (the standard 6-31G(d,p) basis sets for N, C, H, S, O elements) and employing the Windows versions of Gaussian 98 (G98W) [25]. Geometries of complexes **1** and **2** were fully optimized. Multiplicity of the Ni(II) central atom was considered as 1 for all complexes. No symmetry constraints were applied in the calculations. At the same level and basis sets, calculations of natural electron population, natural charge for each atom and frontier molecular orbitals of the compounds have been performed by natural bond orbital (NBO) analysis [26] on the gas phase optimized structures.

3. Results and discussion

The HL and H$_2$L′ Schiff bases of *S*-allyldithiocarbazate have the thioamide function —N(H)C(S) in which the thione form had to be converted to the thiolate form so that the complexation can occur [27]. Although the thione form of the ligands is stable in solid state, it converts to thiolate form in solution and in the presence of metal ions and mild bases [28]. After deprotonation, the ligand L is bidentate (N,S) with charge −1, while L′ is tridentate (O,N,S) with charge −2. So, it is expected that the complex of L with Ni(II), i.e. **1**, is bischelate, while in the case of **2** the complex is formed by one ligand molecule (monochelate tridentate) plus another neutral monodentate ligand molecule (imidazole). The molar conductivities of the complexes in DMF indicate that they are non-electrolyte compounds. Elemental analysis, spectral studies and X-ray crystallography have finally confirmed the structure of these compounds.

3.1. Spectroscopic characterization of complexes

Compound **1:** the v(N—H), v(CSS) and v(C=S) bonds in free ligand at 3105 cm^{-1}, 1334 cm^{-1} and 1097 disappear in complexes spectra that indicating deprotonation of ligand during the complexation [29]. Lowering v(C=N) from 1609 cm^{-1} in the ligand to 1598 cm^{-1} in the nickel complex reveals that azomethine nitrogen is coordinated to metal [29]. The bands at 1640 and 1025 cm^{-1} were assigned for v(N—N) and v(C=C) stretching energy increase.

The ^{1}H NMR spectrum of NiL$_2$ in CDCl$_3$ does not show any peaks at ca. δ 13.33 ppm and 4 ppm attributed to the resonances of N^{2}H and S^{1}H protons, that indicating that the ligand is coordinated in the thiolate form. The upfield shift of the azomethine proton from 7.9 ppm to 8.1 ppm suggests that the coordination occurs via azomethine nitrogen atom of ligand.

The electronic spectrum of the NiL$_2$ complex shows two bands in the 285 and 256 nm regions which can be assigned to the $\pi \rightarrow \pi^*$ transition of the azomethine group and ring, respectively. These bands are observed at 295 and 240 nm in the spectrum of the free ligand. The band at 317 nm can be assigned to the $n \rightarrow \pi^*$ transition of the dithiocarbazate moiety. Bands attributed to this transition appeared at 334 and 345 nm in HL spectrum. In addition, S $\rightarrow$ Ni(II) charge transfer band appeared at approximately 450 nm. In the electronic spectrum of a square-planar nickel complex, it is expected that three bands corresponding to the transition $^1A_{1g} \rightarrow {}^1A_{2g}$, $^1A_{1g} \rightarrow {}^1B_{1g}$ and $^1A_{1g} \rightarrow {}^1E_g$ are seen, but the presence of sulfur covers these bands under its very intense inter-ligand and charge transfer band; hence, the mentioned bands are not observed.

Compound **2:** IR spectral assignment of the complex **2** does not show any medium bands in the regions 3200 and 3097 cm^{-1} due to the v(O—H) and v(N—H) vibrations, respectively, providing strong evidence for ligand coordination around the nickel(II) ion in its deprotonated form. The v(C=N) band at 1595 cm^{-1} show a red shift at about 15 cm^{-1} related to ligand. The coordination of the ligand in the thiolate form is confirmed by the absence of v(C=S) and v(CSS) bands. These peaks are observed at 1319 and 1095 cm^{-1} in the free ligand. No significant change is observed for v(N—N) after coordination. The coordination of phenoxy oxygen to the metal is supported by the increase in v(C—O). Presence of imidazole moiety is confirmed with a peak at 3053 cm^{-1} related to N—H vibration of imidazole.

The ^{1}H NMR spectrum in CDCl$_3$ of compound **2** does not display bands corresponding to NH and SH that confirm the presence of thiolate form of the ligand in the complex.

The electronic spectral data for the H$_2$L′ and complex **2** are recorded in the range of 200–900 nm (CHCl$_3$). The two bands at 243 and 270 nm are attributed to $\pi \rightarrow \pi^*$ of ring and dithiocarbazate moiety respectively. The $n \rightarrow \pi^*$ transition was observed at 383, 351 and 360 nm in the free ligand, but after complexation just a broad band was detected at 383 nm. The intense band at 419 nm is LMCT band. The tail of this band covers all *d–d* transition.

3.2. X-ray structure analysis

Ortep diagrams of **1** and **2** are reported in Figs. 1 and 2 respectively. Selected geometric parameters are given in Table 2. The X-ray analysis confirms that **1** is a bischelate complex of point symmetry C_i, as the nickel atoms lie on crystallographic inversion centres, while **2** is a monochelate complex with an additional neutral ligand (imidazole) coordinated to the metal. The square planar coordination geometry is fairly regular in both the complexes, with the four bond angles around the metal all close to 90°. In particular,
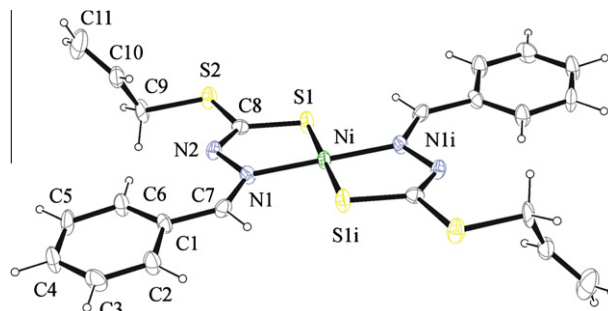

Fig. 1. Ortep diagram of **1**. Thermal ellipsoids are drawn at 50% probability level.
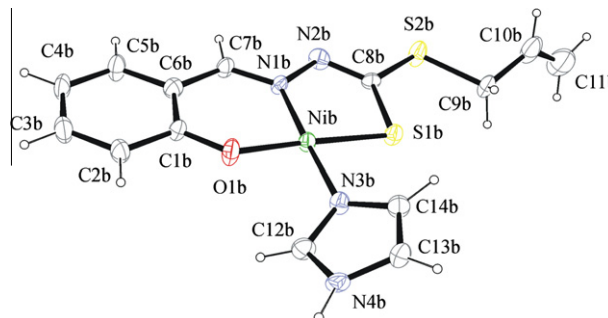

Fig. 2. Ortep diagram of one independent molecule of **2**. Thermal ellipsoids are drawn at 50% probability level.

Table 2
Selected bond lengths (Å) for **1** and **2**, with esd's in parentheses.

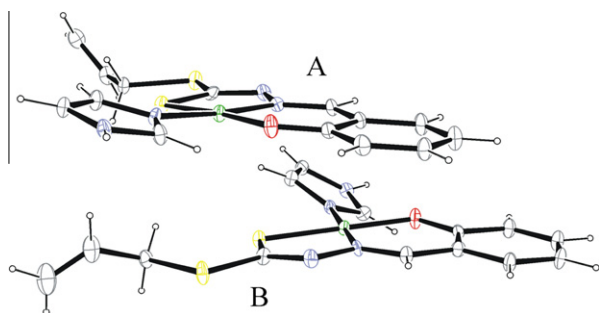| Compound	1		2	
	Experimental	Calculated	Experimental	Calculated
Ni—S1	2.175(2)	2.254	2.149(2), 2.137(2)	2.229
C7—N1	1.300(8)	1.303	1.313(8), 1.286(8)	1.309
N1—N2	1.403(7)	1.338	1.400(7), 1.416(7)	1.387
C8—N2	1.281(8)	1.301	1.294(8), 1.291(8)	1.294
C8—S1	1.722(7)	1.743	1.719(7), 1.719(6)	1.750
C8—S2	1.745(6)	1.767	1.750(7), 1.752(7)	1.779
Ni—N1	1.928(5)	1.948	1.860(5), 1.865(5)	1.883
Ni—N3			1.923(5), 1.915(5)	1.954
Ni—O1			1.853(5), 1.837(5)	1.864

Fig. 3. The two crystallographically independent molecules of **2**.

the bite angles corresponding to the formation of the five-membered rings are slightly contracted (N1—Ni—S1 = 85.7(2)° in **1**, 87.0(2), 86.7(2)° in **2**) and the others slightly enlarged. The metal and the four atoms to which it is bonded are strictly planar in **1** and are planar within 0.069(3) Å and 0.022(3) Å in the A and B independent molecules of **2** respectively. In both the complexes, the metal-to-nitrogen distances are, on average, 0.2 Å shorter than the metal-to-sulfur distances. The inspection of the bond lengths clearly indicates that the coordinated ligand is in the thiolato form in both complexes. This is strongly suggested, in particular, by the bond lengths C7—N1 (1.300(8) Å in **1**, 1.313(8), 1.286(8) Å in **2**) and C8—N2 (1.281(8) Å in **1**, 1.294(8), 1.291(8) Å in **2**) which take values close to those expected for a double bond.

The two crystallographically independent molecules of **2** mainly differ for the orientation of the imidazole ligand with respect to the coordination plane (Fig. 3).

In fact, the dihedral angle between the mean coordination plane and the average plane of the imidazole ligand is 14.7(3)° in the molecule A and 33.4(3)° in B; the different orientation is achieved by torsion around the Ni—N3 bond (Fig. 3). Moreover, the two independent molecules are oriented with their coordination planes very little tilted with respect to each other (the dihedral angle between the mean planes is 8.2(2)°) (Fig. 3).

The conformation of the ligands is different in the two complexes. In fact, the bond C7=N1 is *trans* in **2** while it is *cis* in **1**; this is probably a consequence of the higher steric overcrowding in the bischelate complex **1**. Also the conformation of the allyl group is different in the two compounds. In fact, C9 is *trans* with respect to S1 in **1** while it is *cis* in **2**. So, the overall shape of the ligand is bent in **1**, while it is extended in **2**.

At variance of **1**, whose packing is determined by normal van der Waals contacts, the packing of **2** is conditioned by the formation of H bonds. In particular, molecules in **2** are arranged in chains through H bonding between the N—H donor of the imidazole ligand of a molecule and the N2 acceptor of the other independent molecule. The H bonded chains run parallel to **c** (Fig. 4). According to our previous researches, the presence of allyl moiety in these compounds produces hydrogen interactions, which in turn they play a role in lattice expanding [30,31]. But this effect is just seen in the complex **2** in which hydrogen bonds of S1B···H9A—C9A, C11A···H5A—C5A, C10B···H2A—C14A and C11B···H13A—C13A cause the expansion of crystalline structure. There is not any allyl interaction in the compound **1**. This lack of interaction is seen in some similar cases [32].

In the crystals of **2**, molecules are arranged with their coordination planes approximately parallel to each other and lying on the planes of the family with Miller indices 220 (the reflection 220 is the second most intense of the whole diffraction pattern) (Fig. 5). The Bragg spacing $d_{220} = 3.502$ Å is also the average stacking distance of the molecules along **a** + **b**.

3.3. Geometry optimization, charge distribution and electronic structure

In the complexes, the calculated bond lengths and angles are in a good agreement with the values based upon the X-ray crystal structure data (see Table 2). A difference between the experimental and theoretical studies is that computations were done in the gas phase, whereas the X-ray data was obtained in the solid phase for complexes.

The calculated charges on the nickel atom in complexes (**1** = 0.16 and **2** = 0.36) are considerably lower than the formal charge +2, that confirming a significant charge donation from the ligands. In compound **1**, the calculated Mullikan charge for the atoms S1 and S1i is less than −1 and the electron density in valence 3s and 3p orbitals is lower than the predicted values.

In the complex **2**, the calculated Mulliken charge values for S1 and O are −0.099 and −0.643 respectively, that is less than the
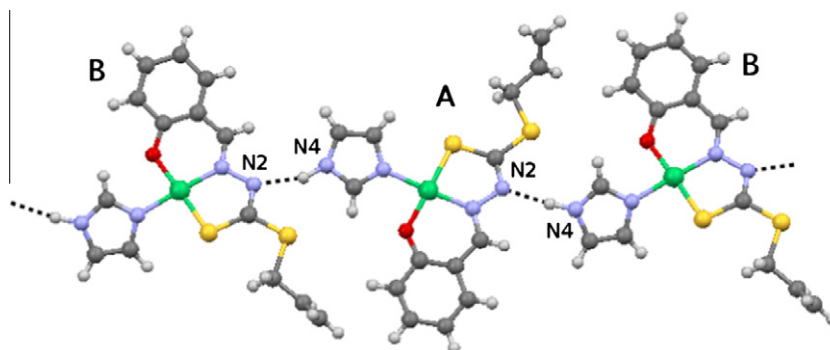

Fig. 4. A chain of H-bonded molecules in **2**. Structural parameters of the H bonds [33]: N4A—H···N2B^i: 1.03 Å, 1.98 Å, 2.971(8) Å, 160.2°, $i = -x, -y, -z$; N4B^{ii}—H···N2A: 1.02 Å, 1.98 Å, 2.982(8) Å, 166.4°, $i = -x, -y, 1 - z$.
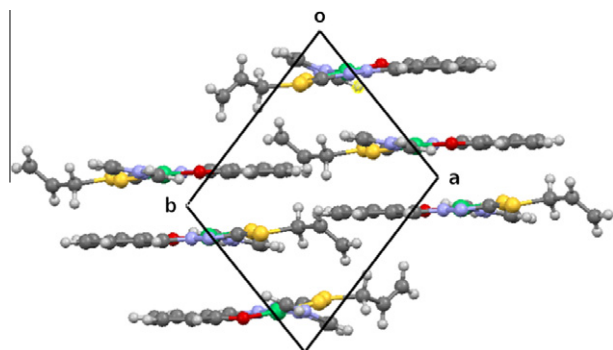
Fig. 5. Crystal packing of **2** viewed down **c**.

formal charge. Similarly, the electron density of these atoms is lower than expected values. All those results indicate electron transfer from the donor atoms to the central metal.

Calculated HOMO and LUMO frontier orbitals of the two complexes are drawn in Fig. 6 and they show relevant differences. In fact, in **1** the HOMO is mainly localized on the phenyl ring, while in the LUMO major contributions come from the metal and, to a lesser extent, from the allyl tail. On the other hand, in **2**, the electron density of the HOMO shows contributions from the whole L′

ligand, from the metal and the imidazole ligand, while in the LUMO the electron density is essentially established on the L′ ligand and, to a lesser extent, on the metal, without relevant contributions from imidazole. Since the first electron transfer occurs from the highest occupied molecular orbital (HOMO) to lowest unoccupied molecular orbital (LUMO), it can be inferred that the first electron transfer in **1** is related to LMCT while in complex **2** the first low energy electronic transition is combined MLCT from metal to organic moiety and intra ligand π → π* electron transition. Additional information on the NBO calculations is presented in Table 3. According to this table, the electron populations on s and p orbitals of oxygen, nitrogen and sulfur donor atoms in both complexes are less than the expected values of valance orbitals, while the computed electron population in central ion in both complexes is more than the expected value in Ni^{+2} with d^8 electron configuration. This confirms the electron transmission of donor atoms toward the central metal.

4. Conclusion

Two Ni(II) complexes derived from bi- and tri-dentate S-allyldithiocarbazates ligands were prepared. The characterization of the complexes was performed in solution by UV and H NMR spectroscopy and in the solid state by single crystal X-ray analysis. Those analyses showed that the HL (N,S) and $H_2L′$ (N,S,O) Schiff
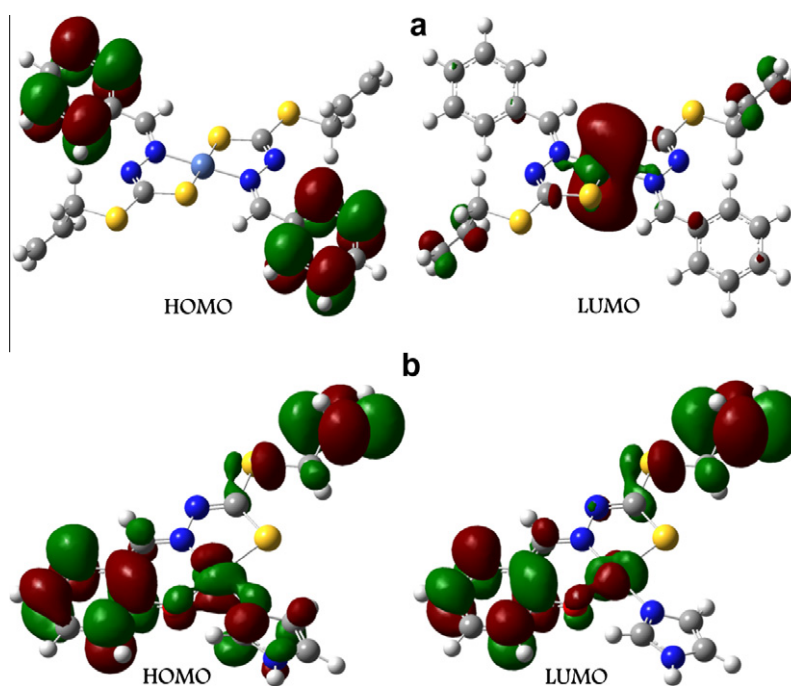

Fig. 6. Calculated HOMO and LUMO for **1** (a) and **2** (b).

Table 3
The natural charges of selected atoms of the studied complexes determined by using of B3LYP/6-31G method.

1			2		
Atom	Charge	Configuration	Atom	Charge	Configuration
Ni	0.164257	[core]4S(0.40)3d(8.87)	Ni	0.364010	[core]4S(0.36)3d(8.78)
Ni	0.164257	[core]4S(0.40)3d(8.87)	Ni	0.364010	[core]4S(0.36)3d(8.78)
S1	−0.086425	[core]3S(1.71)3p(4.34)	S1	−0.098864	[core]3S(1.71)3p(4.38)
S1i	−0.086425	[core]3S(1.71)3p(4.34)	O	−0.642692	[core]2S(1.65)2p(4.99)
N1	−0.303308	[core]2S(1.30)2p(3.93)	N1	−0.329113	[core]2S(1.30)2p(3.97)
N1i	−0.303308	[core]2S(1.30)2p(3.93)	N3	−0.428446	[core]2S(1.33)2p(4.15)

base ligands are coordinated to Ni(II) in their deprotonated forms as bi- and tri-dentate ligands respectively, giving rise to complexes with square-planar coordination geometry.

The small calculated values of the Mulliken charge on nickel atoms in the two complexes confirm donor ability of ligands to nickel(II) centre. Furthermore, HOMO and LUMO studies showed that in NiL_2 and NiL'Im the low energy electronic transition is related to LMCT and combined MLCT and $\pi \rightarrow \pi^*$ respectively.

Acknowledgements

Appendix A. Supplementary material

CCDC 867832 and 867833 contain the supplementary crystallographic data for complexes NiL_2 and NiL'Im respectively. These data can be obtained free of charge via http://www.ccdc.cam.ac.uk/conts/retrieving.html, or from the Cambridge Crystallographic Data Centre, 12 Union Road, Cambridge CB2 1EZ, UK; fax: +44 1223 336 033; or e-mail: deposit@ccdc.cam.ac.uk. Supplementary data associated with this article can be found, in the online version, at http://dx.doi.org/10.1016/j.molstruc.2012.07.018.

References

[1] F.R. Pavan, Eur. J. Med. Chem. 45 (2010) 1898.
[2] S. Kalia, K. Lumba, Dithiocarbazates and their Transition Metal Complexes: Physico-chemical Studies on Some Metal Dithiocarbazates, LAP LAMBERT Academic Publishing, 2010.
[3] S.K.S. Hazari, J. Kopf, D. Palit, S. Rakshit, D. Rehder, Inorg. Chim. Acta 362 (2009) 1343.
[4] M.A. Ali, A.H. Mirza, R.J. Butcher, M.T.H. Tarafder, T.B. Keat, A.M. Ali, J. Inorg. Biochem. 92 (2002) 141.
[5] M.A. Ali, A.H. Mirza, R.J. Butcher, K.A. Crouse, Transition Met. Chem. 31 (2006) 79.
[6] K. Tampouris, S. Coco, A. Yannopoulos, S. Koinis, Polyhedron 26 (2007) 4269.
[7] P. Bera, C.H. Kim, S. Il Seok, Inorg. Chim. Acta 362 (2009) 2603.
[8] M. Yazdanbakhsh, R. Takjoo, Struct. Chem. 19 (2008) 895.
[9] A. Nunez-Montenegro, R. Carballo, E.M. Vazquez-Lopez, Polyhedron 27 (2008) 2867.
[10] R. Takjoo, R. Centore, M. Hakimi, S.A. Beyramabadi, A. Morsali, Inorg. Chim. Acta 371 (2011) 36.
[11] P. Bera, S. Il Seok, J. Solid State Chem. 183 (2010) 1872.
[12] Y.H. Liu, J. Ye, X.L. Liu, R. Guo, J. Coord. Chem. 62 (2009) 3488.
[13] P. Bera, C.-H. Kim, S. Il Seok, Solid State Sci. 12 (2010) 532.
[14] A. Boschi, A. Massi, L. Uccelli, M. Pasquali, A. Duatti, Nucl. Med. Biol. 37 (2010) 927.
[15] L.P. Fabbrizzi, Antonio, Chemistry at the Beginning of the Third Millennium, Springer-Verlag, New York, 2000.
[16] M. Wang, L.F. Wang, Y.Z. Li, Q.X. Li, Z.D. Xu, D.M. Qu, Transition Met. Chem. 26 (2001) 307.
[17] M.A. Ali, A.H. Mirza, M. Nazimuddin, H. Rahman, R.J. Butcher, Transition Met. Chem. 27 (2002) 268.
[18] U. Caruso, R. Centore, B. Panunzi, A. Roviello, A. Tuzi, Eur. J. Inorg. Chem. (2005) 2747.
[19] M. Yazdanbakhsh, M.M. Heravi, R. Takjoo, W. Frank, Z. Anorg. Allg. Chem. 634 (2008) 972.
[20] Bruker-Nonius, SADABS, Delft, The Netherlands, 2002.
[21] A. Altomare, M.C. Burla, M. Camalli, G. Cascarano, C. Giacovazzo, A. Guagliardi, A.G.G. Moliterni, G. Polidori, R. Spagna, J. Appl. Crystallogr. 32 (1999) 115.
[22] G.M. Sheldrick, Acta Crystallogr. A64 (2008) 112.
[23] A.D. Becke, J. Chem. Phys. 98 (1993) 5648.
[24] C. Lee, W. Yang, R.G. Parr, Phys. Rev. B 37 (1988) 785.
[25] M.J. Frisch, G.W.Trucks, H.B. Schlegel, G.E. Scuseria, M.A. Robb, J.R. Cheeseman, V.G. Zakrzewski, J.A. Jr. Montgomery, R.E. Stratmann, J.C. Burant, S. Dapprich, J.M. Millam, A.D. Daniels, K.N. Kudin, M.C. Strain, O. Farkas, J. Tomasi, V. Barone, M. Cossi, R. Cammy, B. Mennucci, C. Pomelli, C. Adamo, S. Clifford, J. Ochterski, G.A. Petersson, P.Y. Ayala, Q. Cui, K. Morokuma, N. Rega, P. Salvadar, J.J. Dannenberg, D.K. Malick, A.D. Rabuck, K. Raghavachari, J.B. Foresman, J. Cioslowski, J.V. Ortiz, A.G. Baboul, B.B. Stefanov, G. Liu, A. Liashenko, P. Piskorz, I. Komaromi, R. Gomperts, R.L. Martin, D.J. Fox, T. Keith, M.A. Al-Laham, C.Y. Peng, A. Nanayakkara, M. Challacombe, P.M.W. Gill, B. Johnson, B., W. Chen, M.W. Wong, J.L. Andres, C.Gonzalez, M. Head-Gordon, E.S. Replogle, J.A. Pople, Gaussian 98, Revision A.11.2, Gaussian, Inc., Pittsburgh PA, 2001.
[26] S. Miertus, E. Scrocco, J. Tomasi, Chem. Phys. 55 (1981) 117.
[27] F.N.F. How, K.A. Crouse, M.I.M. Tahir, D.J. Watkin, J. Chem. Crystallogr. 39 (2009) 894.
[28] M.H.S.A. Hamid, M. Akbar Ali, A.H. Mirza, P.V. Bernhardt, B. Moubaraki, K.S. Murray, Inorg. Chim. Acta 362 (2009) 3648.
[29] R. Takjoo, R. Takjoo, M. Yazdanbakhsh, Chin. J. Chem. 28 (2010) 221.
[30] R. Takjoo, S.W. Ng, E.R.T. Tiekink, Acta Crystallogr. E68 (2012) m1033.
[31] M. Ahmadi, J.T. Mague, A. Akbari, R. Takjoo, Polyhedron 42 (2012) 1569.
[32] R. Takjoo, R. Centore, L. Rhyman, P. Ramasami, J. Coord. Chem. 65 (2012) 1569.
[33] The geometric parameters of the hydrogen bond D–H···A are given, here and throughout the paper, in the following order: D–H (Å), H···A (Å), D···A (Å), D–H···A (°), symmetry code of the acceptor atom.